Earthquake Geotechnical Engineering for Protection and Development of Environment and Constructions – Silvestri & Moraci (Eds)
 ISBN 978-0-367-14328-2

S-wave velocity inversion based on microtremor HVR: Effectiveness of the EMR correction for the Grenoble basin

H. Kawase, F. Nagashima & E. Ito
Disaster Prevention Research Institute, Kyoto University, Kyoto, Japan

C. Cornou
University of Grenoble Alpes, University of Savoie Mont Blanc, CNRS, IRD, IFSTTAR, ISTerre, Grenoble, France

ABSTRACT: The Horizontal-to-Vertical spectral ratios of microtremors (MHVRs) or earthquakes (EHVRs) have been utilized as a convenient tool to extract a predominant frequency. We calculated EMRs, the average ratios of EHVRs with respect to MHVRs, for five categories of sites based on the fundamental peak frequency. Using EMRs we translated MHVRs into pseudo EHVRs (pEHVRs) successfully. The applicability of EMR obtained from one region to the other may not be warranted. So we tried to apply the EMR correction method to the Grenoble basin where both microtremors and earthquakes have already been observed. When we compared pEHVRs with EHVRs, we found that pEHVRs tend to overestimate the observed EHVRs, although the frequency characteristics after the fundamental peak are similar. The difference in the high frequency in pEHVR comes from the high amplitude in EMR, which is probably due to the much softer nature of the average basin structure in Japan in comparison to the Grenoble basin.

1 INTRODUCTION

The Horizontal-to-Vertical spectral ratios of microtremors (MHVRs) have been utilized as a convenient tool to extract a predominant frequency at a target site. The so-called "Nakamura" method (Nakamura, 1989) assumed that MHVRs provided us directly with the S-wave amplification factor of an earthquake in the horizontal components (i.e., HHR). However, based on the diffuse field theory recently proposed by Sánchez-Sesma et al. (2011) and Kawase et al. (2011), MHVRs correspond to the square root of the ratio of the imaginary part of the horizontal displacement for a unit harmonic load and the corresponding one in the vertical direction, while Horizontal-to-Vertical spectral ratios of earthquake (EHVRs) correspond to the ratio of the horizontal motion for a vertical incidence of an S-wave with respect to the corresponding P-wave. Thus, there should be a systematic difference between EHVRs and MHVRs because of the difference in their primary contribution of wave types.

To develop an empirical correction scheme, we have calculated the ratios of EHVRs with respect to MHVR (i.e., EMR) at 100 strong motion stations of K-NET and KiK-net in Japan (Aoi et al. 2000). We then normalized the frequency by the fundamental peak frequency at each site and calculated the average of the EMRs for five categories of sites based on the fundamental frequency. Once we got empirical EMRs for five categories we translated MHVRs into pseudo EHVRs (pEHVRs). When we compare pEHVRs with the real EHVRs it turns out that the similarity between them is quite high, even for the sites where we did not use to calculate EMR.

As a matter of course this empirical EMR correction factors should be a function of the S- and P-wave velocity structures from the bedrock to the surface as the theory suggests, and so the applicability of the EMR factors obtained from one region to the other different regions may not be warranted. Thus we tried here to apply the empirical EMR correction method established in Japan to the observed microtremor data in the Grenoble basin, where both microtremors and earthquake ground motions have already been observed at several sites inside the basin.

2 EMPIRICAL EMR CORRECTION

Motivation for the empirical correction to MHVR in order to get pEHVR is to apply an easier inversion method based on the EHVR, as has been shown in several literatures (e.g., Nagashima et al. 2014, Fukihara et al. 2015, Nagashima et al. 2017), to more easily observable microtremor data. Since the fundamental source of energy for earthquake and microtremors are totally different, the frequency characteristics of MHVR and EHVR could be different, especially after the fundamental peak. Therefore, we proposed a new method in which empirical transformation from MHVR to EHVR can be performed based on the observed spectral ratio between EHVR and MHVR, that is, EMR. EMRs are calculated as the averaged values from observed data for different categories classified based on their fundamental peak frequencies in MHVRs. The resultant HVRs transformed from MHVRs, that is, pEHVRs, show quite similar characteristics to the observed EHVRs and so the inverted structures from pEHVRs are quite similar to those from the observed EHVRs. The details of the method to obtain empirical EMRs and the effectiveness of the EMR correction can be found in Kawase et al. (2017) so that only the essence of the results is reproduced here.

We used K-NET and KiK-net sites in Japan to obtain EMRs, where we observed microtremors at 100 points by our own efforts from 2000 to 2015. Strong motion data at these sites are observed and distributed by NIED (Aoi et al. 2000). Figure 1 shows an example of comparison among a) observed EHVRs for the 40 s window from the onset of the S-wave, b) EHVRs for another 40 s window after that S-wave window, and c) MHVRs for more than 50 extracted windows of 40 s from 15 minutes measurements on the nearby surface of the sites. As we can see the EHVRs for the main S-wave windows and the coda windows are almost identical to each other; this is one piece of evidence for the validity of applying diffuse field theory to the direct S-wave window as long as we are taking averaged HVRs for tens of earthquakes. We should also notice the stability of small fluctuations in S-wave part and coda part in the high-frequency range. This suggests that these small peaks and troughs are the emergence of S-wave amplification between the seismological bedrock and the surface. In contrast MHVRs show different spectral characteristics, especially in the frequency range higher than the fundamental peak frequency, although the fundamental peak frequency and its amplitude are well

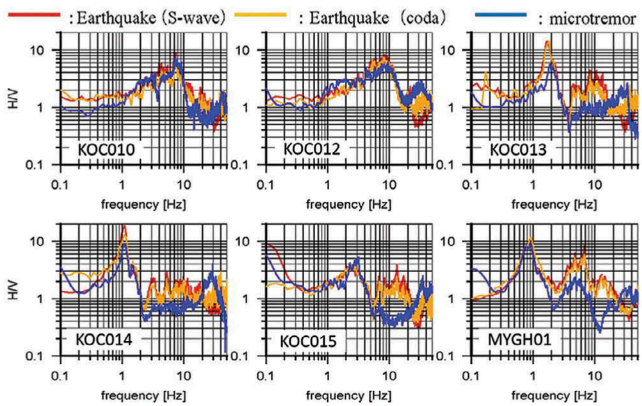

Figure 1. Direct comparison of the average EHVRs of S-wave and S-coda, together with the average MHVRs for microtremors at six sites in Japan.

correlated with those of EHVRs. In general the amplitude level of MHVRs is either the same as or smaller than that of EHVRs.

After the whole analysis of 100 sites we obtained the average EMRs. At first we use just the averaged EMR for all the data but it turns out that the frequency characteristics of EMR is different at the lower and higher frequency sides with respect to the fundamental peak frequency f_p of microtremors. Therefore, we divided 100 sites into 5 categories with f_p for 0.2 to 1 Hz, 1 Hz to 2 Hz, 2 Hz to 5 Hz, 5 Hz to 10Hz, and 10Hz to 20 Hz and normalized EMR by f_p to reflect the common feature around the fundamental peak. Figure 2 shows an average of EMR, together with all the individual EMRs in the five categories with respect to the normalized frequency f/f_p. As we can see at around 1 in the normalized frequency, EMR is close to 1.0 no matter what the category is and EMRs are also close to 1 on the lower frequency side of the categories 1 to 3 but they are close to 1 on the higher side of the category 4 and 5. The maximum amplitude of EMR in the latter is about 2 at around 0.6 in the normalized frequency. On the contrary, the maximum amplitude in the former is about 3 to 4 at around 3 to 10 in the normalized frequency. This means that EMR for a site inside a deep sedimentary basin, which yields a lower fundamental peak frequency, tends to be large in the frequency

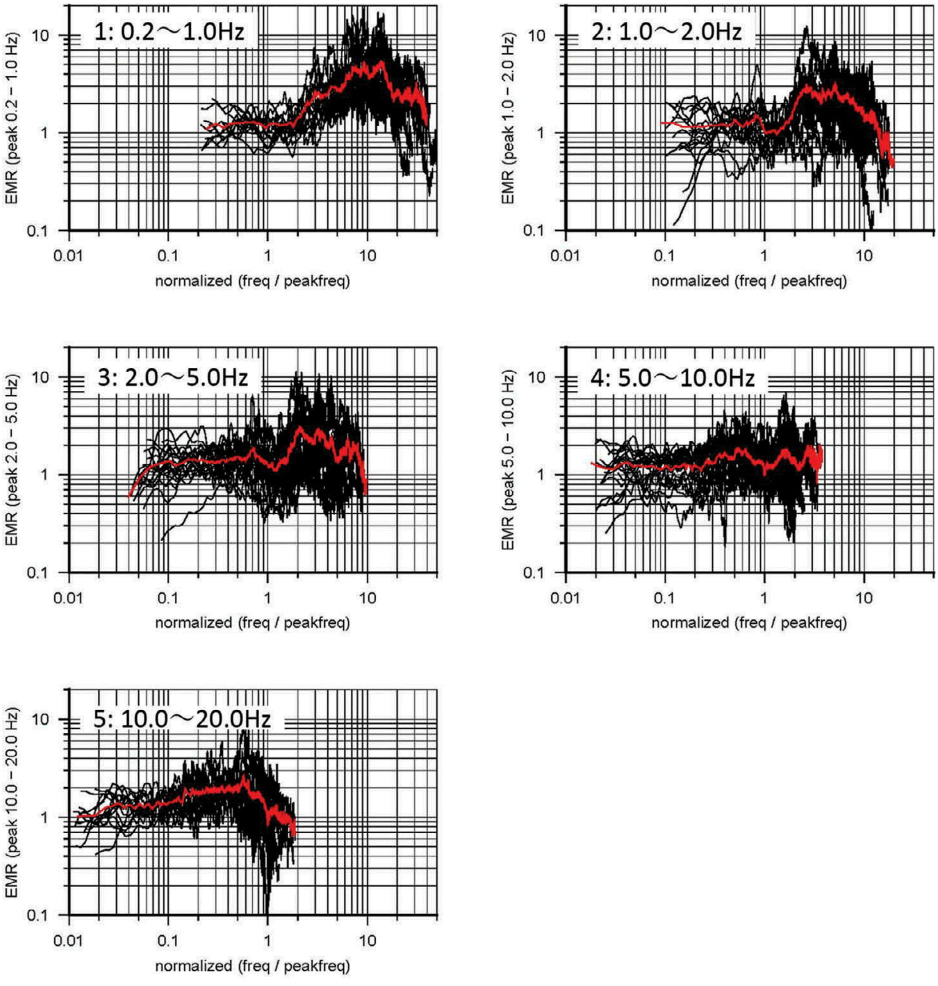

Figure 2. Averaged EMRs (thick red lines) and individual EMRs (thin black lines) for the 100 K-NET and KiK-net sites analyzed for five categories based on the fundamental peak frequency.

range higher than the fundametal peak frequency but that EMR for a site on a hard sediment or rock, which yields a higher fundamental peak frequency, tends to be small in the frequency higher than that and moderate in the frequency lower than that.

3 DATA OF THE GRENOBLE BASIN

3.1 *Earthquake observation network*

In France the French Accelerometric Network (Réseau Accélérométrique Permanent, RAP) has been operating since 1995. About 150 stations cover the national French territory providing high quality data, even for small events, which is freely available through the website RESIF/RAP: https://rap.resif.fr/(Pequegnat et al., 2008). We use all the data provided through the ORFEUS/EIDA seismic data distribution site (http://www.orfeus-eu.org/data/eida/). There are eight permanent seismic stations inside the Grenoble basin as shown in Figure 3.

As we can see in the EHVRs calculated at these eight sites, the fundamental peak frequencies at the sites inside the basin are at around 0.3 to 0.45 Hz. GRN, OGMU, and OGIM did not show high amplitude peaks in the frequency range lower than 1.0 Hz, which suggests their shallow depth of sediments (OGIM) or weathered rock formation down to the bedrock (OGMU, GRN).

3.2 *Microtremor measurements*

For the microtremor measurement several French projects performed a variety of measurements in the past (e.g., SESAME project, Bard et al. 2004). Also theoretical 2D/3D basin responses based on the velocity structure constructed by various geophysical methods confirmed the validity of the model (e.g., Cornou et al. 2004, Chaljub et al. 2006). The wrap-up work based on the large numbers of microtremor observation were reported by Guéguen et al. (2007), where the contour map of MHVR peak frequency is shown in the major portion of the Grenoble basin, which is reproduced here as Figure 5. It shows a nice correspondence with the peak frequency of EHVRs at five sites shown in Figure 4 (triangles with peak frequency in the right panel).

In Figure 6 we show two examples of MHVRs inside the northeastern side of the basin. We can see nice fundamental peak in the frequency range well below 1 Hz. We also note that we have no significant peak or peaks in the frequency range higher than the fundamental peak frequency.

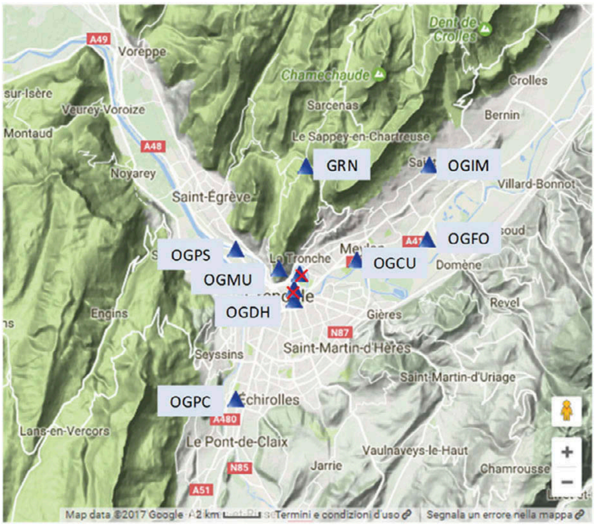

Figure 3. Seismic observation stations in Grenoble.

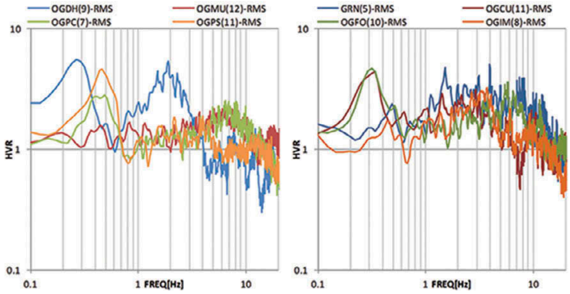

Figure 4. Calculated EHVRs at eight sites in Grenoble. Numbers of earthquakes are shown in parentheses.

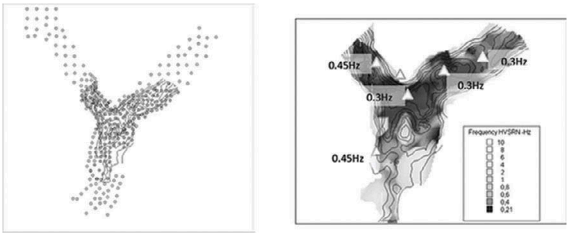

Figure 5. Locations of the microtremor observation sites with the basin depth contour lines (100m each) from the gravity measurement (left) and the contour map of the peak frequency in MHVR (reproduced from Guéguen et al. 2007). Triangles are locations of six earthquake observation sites.

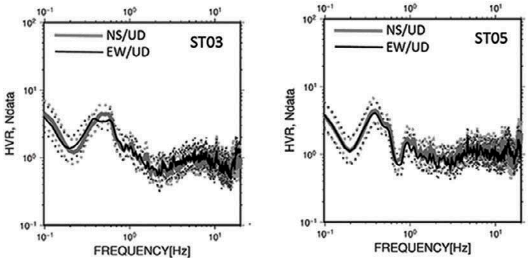

Figure 6. Two examples of MHVR inside the Grenoble basin.

4 INVERSION ANALYSIS USING EHVR AND MHVR

4.1 *Earthquake HVR inversion*

Based on the diffuse field theory for earthquake, EHVR is proportional to the horizontal-to-vertical ratio of the amplification factor between seismic bedrock and the ground surface as shown in Equation 1.

$$\frac{H}{V} = \sqrt{\frac{\alpha}{\beta}} \frac{|TF_{horizontal}|}{|TF_{vertical}|} \tag{1}$$

where α = P-wave velocity (Vp) at the seismic bedrock; β = S-wave velocity (Vs) at the seismological bedrock (i.e., the half-space with a source); and TF = transfer function of the surface motion due to the vertically incident S-wave (horizontal) or P-wave (vertical) at the seismological bedrock (Kawase et al., 2011). The square root of the velocity ratio is coming from the equipartition of energy in the half-space. We should note that this is the equation for a single-component or an RMS value, not for the vector sum of two horizontal components. We minimized the residuals between the observed EHVR and the theoretical ratio in Equation (1) to identify the subsurface structure down to the seismological bedrock. We use RMS values for horizontal components.

In our inversion using EHVR, the identified valuables were Vs, Vp and thickness of all layers except for the half space, and the damping factor *h* was assumed to be 1.1% (Q=45) for all layers. The mass density was converted from Vs. We applied the so-called hybrid heuristic search combined Genetic Algorithm and Simulated Annealing to find the optimum structure which can explain the observed EHVR most. The details of our inversion scheme can be found in Nagashima et al. (2014) and Nagashima et al. (2019). Since our method uses a random number to generate the first generation genes (the initial set of model parameters), it gives us slightly different results at every different identification. Therefore, we identified the structure ten times using the same parameter set, then chose the minimum misfit model among these ten results as the best model.

In Figure 7 comparisons of theoretical EHVRs obtained by the inverted structures with the observed EHVRs at three sites in Grenoble, namely OGDH, OGMU, and OGPS are shown. It can be seen that it is possible to identify structures at these sites, especially at the sites inside the basin, and it is possible to reproduce observed EHVRs quite well. The differences among different trials are quite small, suggesting the stability of the inversion, which means sufficient constraint by the observation.

In Figure 8 we plot the S-wave velocity structures identified by EHVR inversions at these three sites. As we can see the velocity structures at OGDH located in the center of the valley should have a soft quaternary layer down to 20 to 25 meters, then several hundreds of meters of basin layers until we reach the hard rock formation with the S-wave velocity higher than 2.0 km/s. On the other hand, at OGPS the sedimentary soil and rock formations above the basin bottom tend to have much higher velocities. At OGMU high velocity layers exist up to

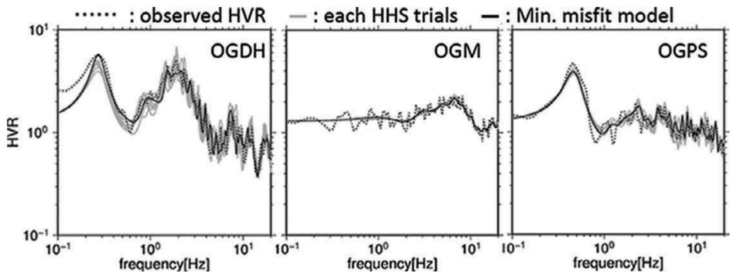

Figure 7. Observed EHVR and theoretical EHVRs obtained by the inversion at three sites.

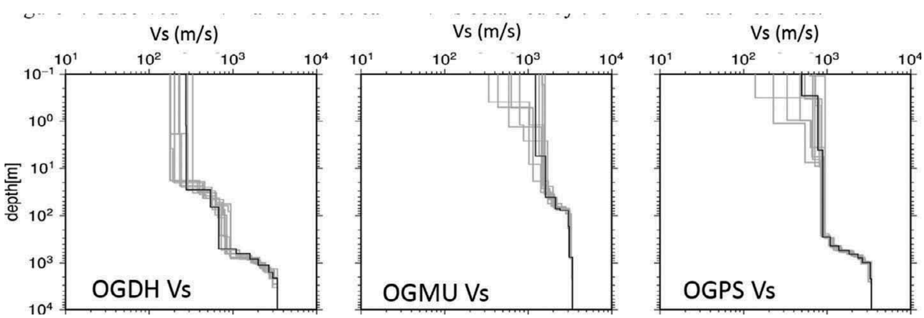

Figure 8. Inverted velocity structures at three sites.

the surface which is the direct consequence of the peak only in the high frequency range (Figure 7). Note that the bedrock velocity is fixed to be 3.4 km/s. This inversion has been done without any “a prior” information and so in the near future we may refer to the velocity structures derived from noninvasive investigations reported recently by Hollender et al. (2018).

4.2 *Microtremor HVR inversion with Japanese EMR*

Finally we use microtremor data together with the empirical correction factor EMR to transform MHVRs into pEHVRs. First we use G-series measurement data (Chaljub et al. 2006) because they are relatively recent measurements and so looks reliable in the lower frequency range. Figure 9 shows three examples of observed MHVRs along the line perpendicular to the basin axis on the northeastern side. We can see that significant amplitude increase is applied to the high frequency part of the MHVRs. When we compared pEHVR to EHVR at the G04 site, which is shown in Figure 10 (right and middle), these amplitude corrections by EMR seems too large.

By using pEHVR we can invert velocity structures at these G-series sites. Figure 10 (right) shows an example at G04. The inverted structure, which has a basin depth at about 550 m, show a good match to the pEHVR on the average. However, this structure may not be a true structure since the real EHVR (Figure 10 left) shows a smaller amplitude in the high frequency range, which will require smaller impedance contrast near the interface to the seismological bedrock.

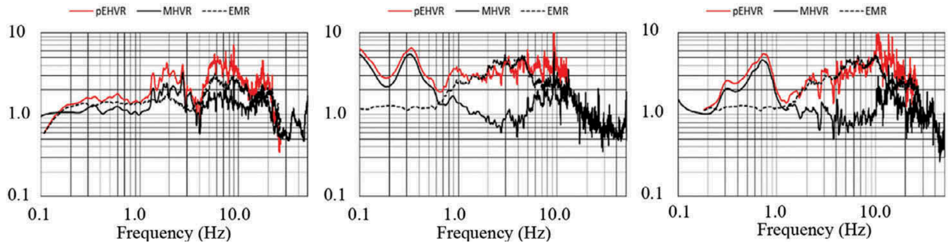

Figure 9. MHVR, EMR, and pEHVR=MHVR*EMR at three sites across the basin.

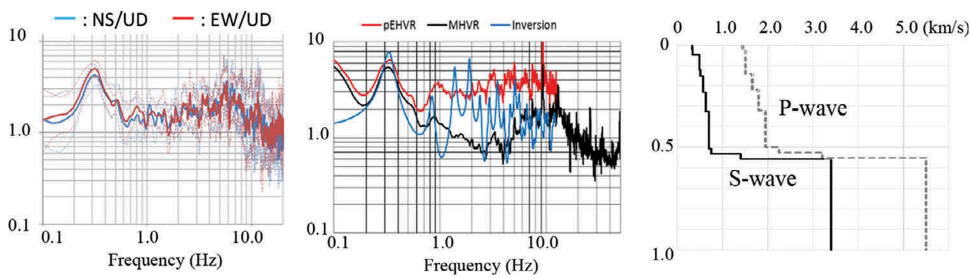

Figure 10. The observed EHVRs from two components (left), pseudo EHVR, MHVR, and theoretical EHVR after inversion (middle), and inverted S- and P-wave velocity structures (right) at G04.

5 CONCLUSION

First we introduced our construction procedure of EMR to transform MHVR into pEHVR. Since general applicability of EMR is not warranted, we tried to apply our EMR correction method to the data in the Grenoble basin. When we compared pEHVR with EHVR in Grenoble, we found that pEHVR tends to overestimate the observed EHVR, although the frequency characteristics after the fundamental peak are similar. We inverted S-wave velocity structures by using pEHVR, instead of EHVR, to find that the resultant velocity values tend to be smaller than those from EHVR. The difference in the high frequency amplitude in pEHVR comes from the high amplitude in EMR in category 1, which is probably due to the much softer nature of the basins in Japan. Thus we may conclude here that we need to adjust the EMR correction factor from region to region. We are currently expanding our analyses to cover the whole region of the basin.

ACKNOWLEDGMENTS

We would like to thank the National Research Institute for Earth Science and Disaster Prevention for allowing us to access to K-NET and KiK-net earthquake data and RESIF - Réseau Sismologique et géodésique Français, Seismic Network, doi:10.15778/RESIF.RA, http://data.datacite.org/10.15778/RESIF.RA for RAP Network data in Grenoble. These Grenoble permanent network data were downloaded through ORFEUS/EIDA data distribution website at http://www.orfeus-eu.org/data/eida/. Figure 3 used Google Map at https://maps.google.com/.

REFERENCES

Aoi S., Obara K., Hori S., Kasahara K. & Okada Y. 2000. New strong-motion observation network: KiK-net. *Eos Transactions, AGU* 81: 329.

Bard, P.-Y. & SESAME PARTICIPANTS. 2004, The SESAME project: an overview and main results, in*Proc. 13th World Conf. Earth. Eng*., Vancouver, Canada, August 2004, Paper # 2207.

Chaljub, E., Cornou, C., Verbeke, J., Converset, J., Voisin, C., Stehly, L., Margerin, L., Tsuno, S., Grasso J.-R., Guéguen, P., Roussel, S., Roux, P., Hatton, S., & Campillo, M. 2006. Measurement and variability study of site effects in the 3D glacial valley of Grenoble, French Alps,*3rd Int. Sym. Effects of Surface Geology on Seismic Motion*, Grenoble, France, August 30-September 1, 2006. Paper Number 154.

Cornou, C., Kristek, J., Ohrnberger, M., Di Giulio, G., Schissele, E., Guillier, B., Boonefoy-Claudet, S., Wathelet, M., Faeh, D., Bard P.-Y., & Moczo, P. 2004. Simulation of seismic ambient vibrations – II H/V and array techniques for real sites, in *Proc. 13th World Conf. Earth. Eng*., Vancouver, Canada, August 2004, paper #1130.

Fukihara K., S. Matsushima, and H. Kawase. 2015. Identification of the velocity structure model of Kyoto Basin for strong motion prediction using observed earthquake and microtremor motions, *J. of JAEE*, 15(6): 60–76. (in Japanese with English abstract).

Hollender, F., C. Cornou, A. Dechamp, K. Oghalaei, F. Renalier, E. Maufroy, C. Burnouf, S. Thomassin, M. Wathelet, P.-Y. Bard, V. Boutin, C. Desbordes, I. Douste-Bacqué, L. Foundotos, C. Guyonnet-Benaize, V. Perron, J. Régnier, A. Roullé, M. Langlais, & D. Sicilia. 2018. Characterization of site conditions (soil class, VS30, velocity profiles) for 33 stations from the French permanent accelerometric network (RAP) using surface wave methods, *Bull. Earthquake Eng.*, 16, 2337–2365, doi:10.1007/s10518-017-0135-5

Kawase H., Sánchez-Sesma, F. J. & Matsushima S. 2011. The optimal use of horizontal-to-vertical spectral ratios of earthquake motions for velocity inversions based on diffuse-field theory for plane waves, *Bull. Seism. Soc. Am.*, 101: 2011–2014.

Kawase, H., Y. Mori & F. Nagashima. 2017. Difference of horizontal-to-vertical spectral ratios of observed earthquakes and microtremors and its application to S-wave velocity inversion based on the diffuse field concept, *Earth, Planets and Space*, 70:1, doi:10.1186/s40623-017-0766-4

Nagashima F., Matsushima S., Kawase H., Sánchez-Sesma, F. J., Hayakawa T., Satoh T. & Oshima M. 2014. Application of horizontal-to-vertical (H/V) spectral ratios of earthquake ground motions to identify subsurface structures at and around the K-NET site in Tohoku, Japan, *Bull. Seism. Soc. Am.* 104: 2288–2302.

Nagashima, F., H. Kawase, & S. Matsushima. 2017. Estimation of horizontal seismic bedrock motion from vertical surface motion based on horizontal-to-vertical spectral ratios of earthquake motions, *Proc 16th World Conf. Earth. Eng*., Santiago Chile, January 9–13, 2017, Paper N°3685.

Nakamura Y. 1989. A method for dynamic characteristics estimation of subsurface using microtremor on the ground surface, *Railway Tech. Res. Inst., Q. Rep*. 30(1): 25–30.

Nagashima F. & H. Kawase. 2019. S-wave and P-wave velocity structure identification based on Horizontal to Vertical spectral ratio and Surface to Borehole spectral ratio of earthquake,*Proc. of 7th ICEGE*, this issue, paper id: 10925 (in print).

Pequegnat, C., Guéguen, P., Hatzfeld, D., & Langlais, M., 2008. The French Accelerometric Network (RAP) and National Data Center (RAP-NDC), *Seismol. Res. Lett*., 79(1), 79–89.

Sánchez-Sesma F.J., Rodríguez M., Iturrarán-Viveros U., Luzón F., Campillo M., Margerin L., García-Jerez A., Suarez M., Santoyo M.A. & Rodríguez-Castellanos A. 2011. A theory for microtremor H/V spectral ratio: Application for a layered medium, *Geophys. J. Int. Exp. Lett*., 186: 221–225, doi: 10.1111/j.1365-246X.2011.05064.x.